The Foot 39 (2019) 1–10

Contents lists available at ScienceDirect

The Foot

journal homepage: www.elsevier.com/locate/foot

Original Article

Electronic measurement of plantar contact area during walking using an adaptive thresholding method for Medilogic® pressure-measuring insoles

Daniel E. Lidstone[a,*], Jessica DeBerardinis[b], Janet S. Dufek[a], Mohamed B. Trabia[b]

[a] Department of Kinesiology and Nutrition Sciences, University of Nevada Las Vegas, USA
[b] Department of Mechanical Engineering, University of Nevada Las Vegas, USA

ARTICLE INFO

Keywords:
Gait
Pressure-measuring insole
Contact area
Optical pedography
Adaptive threshold
Fixed threshold

ABSTRACT

Background: Pressure-measuring insoles have the potential to measure plantar contact area (PA) during walking. However, they are not widely used for this purpose because of the need for a reliable process that can convert the insole output into PA. The purposes of this study were to: (1) develop an *adaptive-threshold* method for pressure-measuring insoles that can improve the accuracy of the PA measurements during walking, and (2) experimentally assess the accuracy and generalizability of this method.

Methods: A sample of 42 healthy, ambulatory, young adults (age = 24.3 ± 3.2 years, mass = 67.2 ± 16.9 kg, height = 1.63 ± 0.08 m) completed 10 trials walking on an elevated walkway while wearing Medilogic® pressure-measuring insoles (sizes 35–45). A total of six insole sizes were considered. Insole data were converted to PA using three unique *adaptive-thresholds* that were based on percentages of the maximum sum of digital values (MSDV) during an analyzed step. Three values were considered: 0.1%, 0.2%, and 0.3% of the MSDV. Additionally, a *fixed-threshold*, which is typically used to estimate PA, was assessed. These two techniques, applied to the insole worn on the left foot, were compared with PA obtained from high-resolution reference footprints obtained from optical pedography of the right foot and processed using digital image processing algorithms. An assumption of PA symmetry between the left (*insole*) and right (*barefoot*) feet was made and comparisons were conducted over the entire stance phase of walking. The generalizability of the algorithm was assessed by comparing PA errors from insoles with respect to the optical pedography results based on insole size criteria.

Results: The *adaptive-thresholds* of 0.1%, 0.2%, and 0.3% of MSDV produced mean errors of 7.31 ± 17.44%, −8.62 ± 15.01%, and −20.45 ± 14.18%, respectively. Using the 2-digital value *fixed-threshold* produced a mean error of 20.88 ± 22.44%. The best performing *adaptive-threshold* varied among insole sizes.

Conclusion: It was observed that the *fixed-threshold* technique produced large magnitudes of errors. The proposed *adaptive-thresholds* of 0.1% and 0.2% of the MSDV reduced PA error to ± 10% during walking. The *adaptive-threshold* method consistently reduced PA error vs. the *fixed-threshold* for each insole size.

1. Introduction

Foot postures, such as pes cavus (high arch) and pes planus (flat foot), are prevalent in community dwelling older adults (5.2% and 19%, respectively) [1] and older adults with diabetes (24.1% and 18.6%, respectively)[2]. Pes cavus and pes planus foot structures lead to elevated plantar pressures that increase risk for lower extremity injury [3], lower extremity pain [4,5], and foot deformities [2]. Furthermore, compared to normal foot structure, pes cavus and pes planus feet show reduced and increased plantar contact area (PA), respectively [6,7]. To use PA as a diagnostic tool of foot structure, valid and reliable methods for identifying the PA are needed. Although PA can be obtained both statically or during walking, dynamic footprint indices can provide a more complete assessment of foot function compared to static footprint indices [8–11].

Simple pedography techniques to measure the PA during walking include ink-mat [12–18] and paper [6,15–17,19]. While these techniques are easy to use and of limited cost, their main disadvantage is that only a single footprint, representing the maximal PA, is obtained. They are unsuited for monitoring changes in PA during walking as several separate footprints from various instances during the stance period are needed to quantify the changes of the footprint over time. This process is time intensive and could not be obtained using a natural gait pattern.

The above deficiency is addressed by optical pedography combined

* Corresponding author at: Department of Kinesiology and Nutrition Sciences, University of Nevada, 4505 S. Maryland Parkway Box 453034, Las Vegas, USA.
E-mail address: daniel.lidstone@unlv.edu (D.E. Lidstone).

https://doi.org/10.1016/j.foot.2019.01.009
Received 25 June 2018; Received in revised form 15 January 2019; Accepted 16 January 2019

Fig. 1. Elevated walkway.

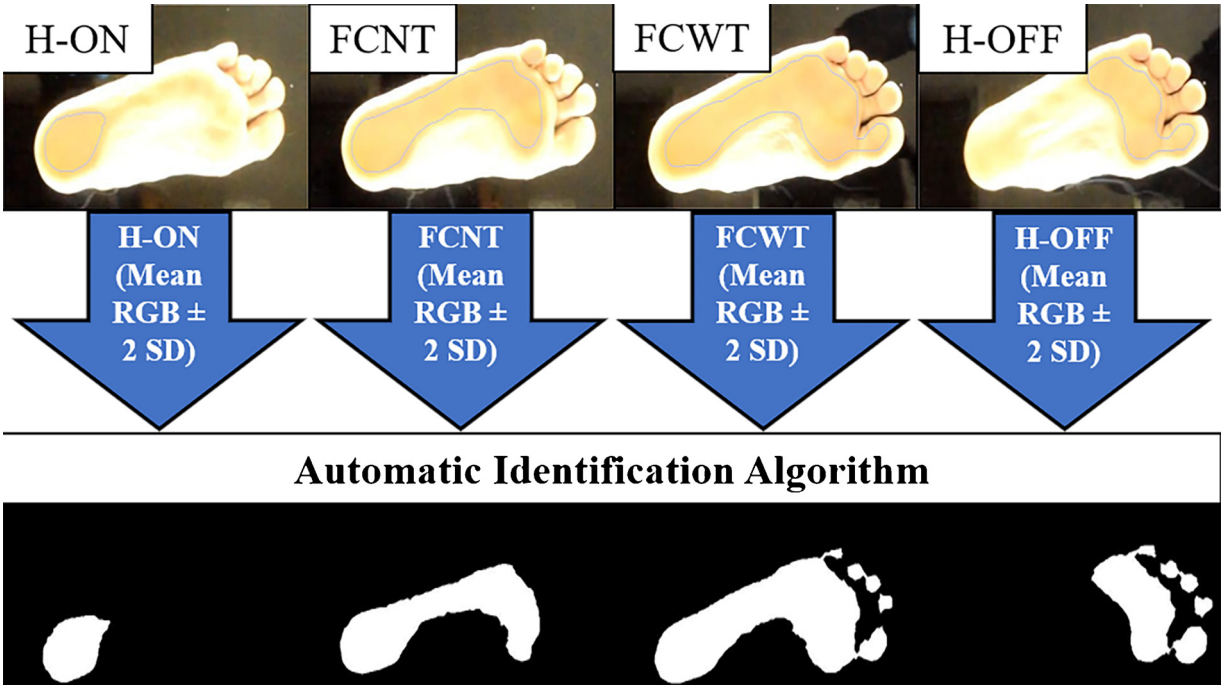

Fig. 2. Optical pedography method including (1) PA phases (heel-on = H-ON, full contact with no toes = FCNT, full contact with toes = FCWT, and heel-off = H-OFF) and (2) automatic identification of contact area.

with digital image processing techniques [20–30]. This technique allows the plantar surface of the foot to be recorded by a digital camera located underneath a transparent platform, typically made of acrylic. Digital image processing techniques are then used to segment the footprint from the background. This technique has several advantages including the ability to assess progressive PA changes over the entire stance phase of walking and high capture rates. Disadvantages of this technique include a lack of standardized methods to identify the footprint using digital image processing algorithms, cumbersome data processing, and limited portability.

Recently, some researchers used various electronic pedography techniques [6,14–17,31] to evaluate PA during walking. These techniques are able to measure the PA and the associated normal ground reaction force component over multiple steps in various locations. However, these pressure-measuring devices rely on a grid of sensors whose accuracy varies between and among devices [32] and the spatial resolution of the sensor grid [13,33]. Bending of the insoles [34] and hysteresis of sensors [35] introduce factors that may increase pressure-

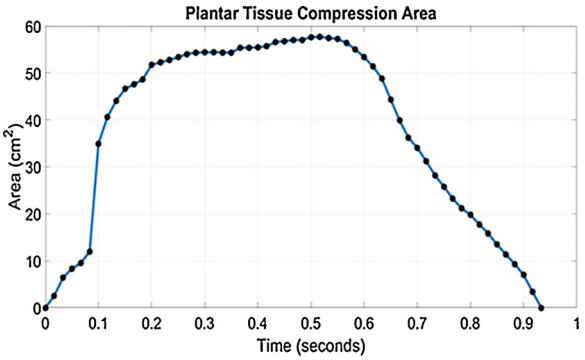

Fig. 3. PA curve from optical pedography method.

measurement and PA error during walking.

Current insole PA measurement techniques involve recording plantar pressures and identifying active sensors above a *fixed-threshold* [16,32,36,37]. However, this technique may not be appropriate for measuring the PA during walking since pressure measurement errors may increase proportionately with the load applied to the sensors. In the current study, an alternative *adaptive-threshold* approach that adjusts the threshold value to the maximal digital value output from the insole during walking is proposed.

The purpose of this study was to (1) develop an *adaptive-threshold* method for pressure-measuring insoles to improve the accuracy of the PA measurements during walking, and (2) experimentally assess the accuracy and generalizability of this method. It was hypothesized that an *adaptive-threshold* method would be more effective at reducing PA error compared to the use of a *fixed-threshold*. The results of the proposed electronic pedography method on the left foot were compared to the corresponding optical pedography technique on the right foot to assess its accuracy. An assumption of PA symmetry between the left (*insole*) and right (*barefoot*) feet was made and comparisons were conducted over the entire stance phase of walking.

2. Material and methods

2.1. Participants

A sample of 42 healthy, ambulatory, young adults (age = 24.3 ± 3.2 years, sex (male/female) = 15/27, mass = 67.2 ± 16.9 kg, height = 1.63 ± 0.08 m) gave the researchers institutionally-approved written consent (IRB protocol 772154-6). All participants were free from lower extremity injuries and obvious foot deformities, as reported by the participants and observed by the research team. Age, mass, height, and insole size were obtained from all participants.

2.2. Pressure-measuring insoles

Medilogic® (Schönefeld, Germany, 60 Hz) pressure-measuring insoles were used in the current study. The number of sensors on the Medilogic® insoles ranges between 93 and 162 sensors depending on the size. Each sensor is a 0.75 × 1.5 cm rectangle (1.125 cm^2) and outputs pressure using an 8-bit converter covering a range of digital values from 0–255. The insole manufacturer states that the 255 digital value is equal to 64 N/cm^2 and that the sensor output is linear [38].

2.3. Elevated walkway

All walking trials were collected on a custom-built elevated acrylic walkway (2.54 cm thick, 1.21 m long, 0.6 m wide, 0.9 m height) (Fig. 1). Acrylic is known to have a low refraction index [39] and high modulus. A stress analysis of the custom acrylic platform determined a maximum deflection of 1.25 mm assuming a 90 kg individual placing their heel in the middle of the plate. A digital camera (Nikon 1®, J4 model, Tokyo, Japan) was used in all experiments. The camera, which produced images of 1920 × 1080 pixels at a rate of 60 frames per second, was placed below the center of the acrylic walkway. The camera was placed in customized 3-D printed housing at a marked location on the ground, 0.9-m below the acrylic platform, for internal consistency. Plantar pressures from each sensor on the left foot were recorded simultaneously at 60 Hz using Medilogic® software to determine left foot PA. The PA from the bare right foot was measured using a previously validated optical pedography technique [40]. Therefore, PA from both the right and the left foot were recorded simultaneously at the same sampling rate (60 Hz) during each walking trial using two separate techniques:

(1) *left foot* — pressure-measuring insole
(2) *bare right foot* — optical pedography.

PA measured over the stance phase of a left foot step was then compared to the PA measured over the stance phase of a right foot step to calculate PA error for each trial. A detailed explanation of the pressure-measuring insole and reference optical pedography technique are found in the following sections.

Pre-processing procedures and data extraction from the optical pedography algorithm are briefly presented in this section (Fig. 2). Optical pedography footprints for the stance phase of walking were generated for each trial using a custom automated identification algorithm. The algorithm was based on the observation that when the plantar tissues are compressed they blanch in comparison to the remainder of the foot, producing a change in coloration of the PA. The concurrent validity of the automated identification algorithm was examined in a separate experiment [40]. The automated identification algorithm showed strong agreement with a reference manual

Fig. 4. Foot placement on insole and insole inserted within sock.

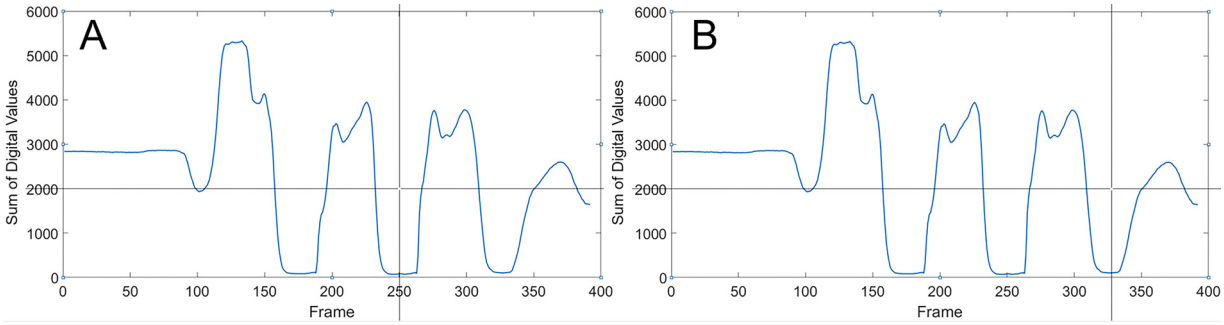

Fig. 5. Identification of the beginning (A) and end (B) of the second step.

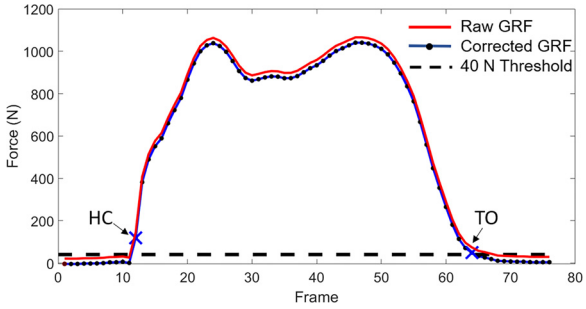

Fig. 6. Processing of the normal component of the ground reaction force (GRF) during stance phase. Heel contact (HC) and toe-off (TO) are identified using the 40 N threshold using the corrected GRF curve.

planimetric tracing method (ICC = 0.939).

It was observed that the stance period has four phases: (1) Heel Contact, (2) Full Contact with No Toes, (3) Full Contact With Toes, and (4) Heel Off. A reference image was chosen from each phase using the criteria below.

1. Heel Contact: frame when the entire heel was in contact with the acrylic platform without any midfoot contact.
2. Full Contact with No Toes: frame when the entire foot was in contact with the platform without any toe contact.
3. Full Contact with Toes: frame when the entire foot, including the toes, were in contact with the platform.
4. Heel Off: frame when the entire heel was elevated off the platform leaving only the forefoot in contact.

This approach, using multiple reference images, was used because the color of the plantar contact area changed at each phase. In addition to selection of a single reference image for each phase of stance, the frame numbers corresponding to the start and end of each phase were identified. Further details can be found in Ref. [40].

For each reference image selected, a contour was drawn along perimeter of plantar contact area and the mean Red–Green–Blue (RGB) ± twice the standard deviation (SD) was calculated for each phase. These RGB ranges were used as to identify the pixels that were part of the PA. Pixels identified as a part of the plantar contact area were summed for each footprint and converted to area (cm^2) using a conversion factor obtained from calibrating the camera. An exemplary area–time curve for the stance phase of walking for a single trial is shown in Fig. 3.

2.4. Experimental protocol

Participants were fitted with tight-fitting black clothing and black nitrile gloves to reduce interference of body parts, other than the foot, during image processing. The right foot of each participant was bare-foot for the entire procedure, to measure PA using the optical pedography technique [6,16,36,41], and a pressure-measuring insole recorded pressures from the left foot. The spatial resolution using the optical pedography method for the right foot was 1 pixel equals 0.0016 cm^2, whereas the spatial resolution of the pressure-measuring insole on the left foot was 1 sensor equals 1.125 cm^2. Insoles were selected based on participant shoe size. In cases where plantar surface of the toes was not covered by the insole, the next largest size was selected (Fig. 4). To simulate barefoot walking, the insoles were placed inside thin socks provided by the researchers [42].

Participants were asked to perform 10 non-recorded practice trials and were instructed to perform the following sequence of steps: (1) step on the walkway with their right foot first, (2) walk along a straight line at a normal pace, (3) keep their eyes focused ahead, and (4) maintain a similar stride and cadence across all the trials. The starting position was adjusted during the practice period so that the right foot contacted the center of the acrylic portion of the walkway naturally. The position of the left foot was not adjusted to be imaged by the video camera since the pressure-measuring insoles worn on the left foot were used to provide a measure of PA. Foot contact directly above the camera, in the center of the camera field of view, also reduced the effects of image distortion on PA measurements. Following the practice period, this starting position was marked with tape to ensure a consistent starting position for each of the subsequent trials.

Each participant then performed 10 recorded walking trials on the walkway. After trial completion, the insole sensor raw data, in 0–255 digital values, were exported as comma separated values (CSV) for post-processing.

2.5. Data processing

Optical pedography footprint processing procedures — The automated identification optical pedography algorithm was used to calculate the PA for all frames during the stance phase of walking. Please refer to Ref. [40] for a detailed outline of processing procedures for the automated identification algorithm. Of the 420 collected trials, 17 trials were removed due to poor video quality.

Pre-processing of pressure-measuring insole data — All processing presented in this work was performed in MATLAB (version 2017a, Natick, MA) as follows:

1. For each trial, 0–255 digital values from all sensors were summed and plotted versus time (Fig. 5).
2. The second step of each trial was manually cropped, using a cross hair tool, by manually selecting a single time point before heel contact and after toe off (Fig. 5).
3. The sum of digital values at the start and end points, that were manually selected by the experimenter, were averaged and subtracted from the time-series. This approach was used to eliminate error due to signals of sensors that were active while not in contact (Fig. 6).
4. To identify heel contact (HC) and toe off (TO), the corrected

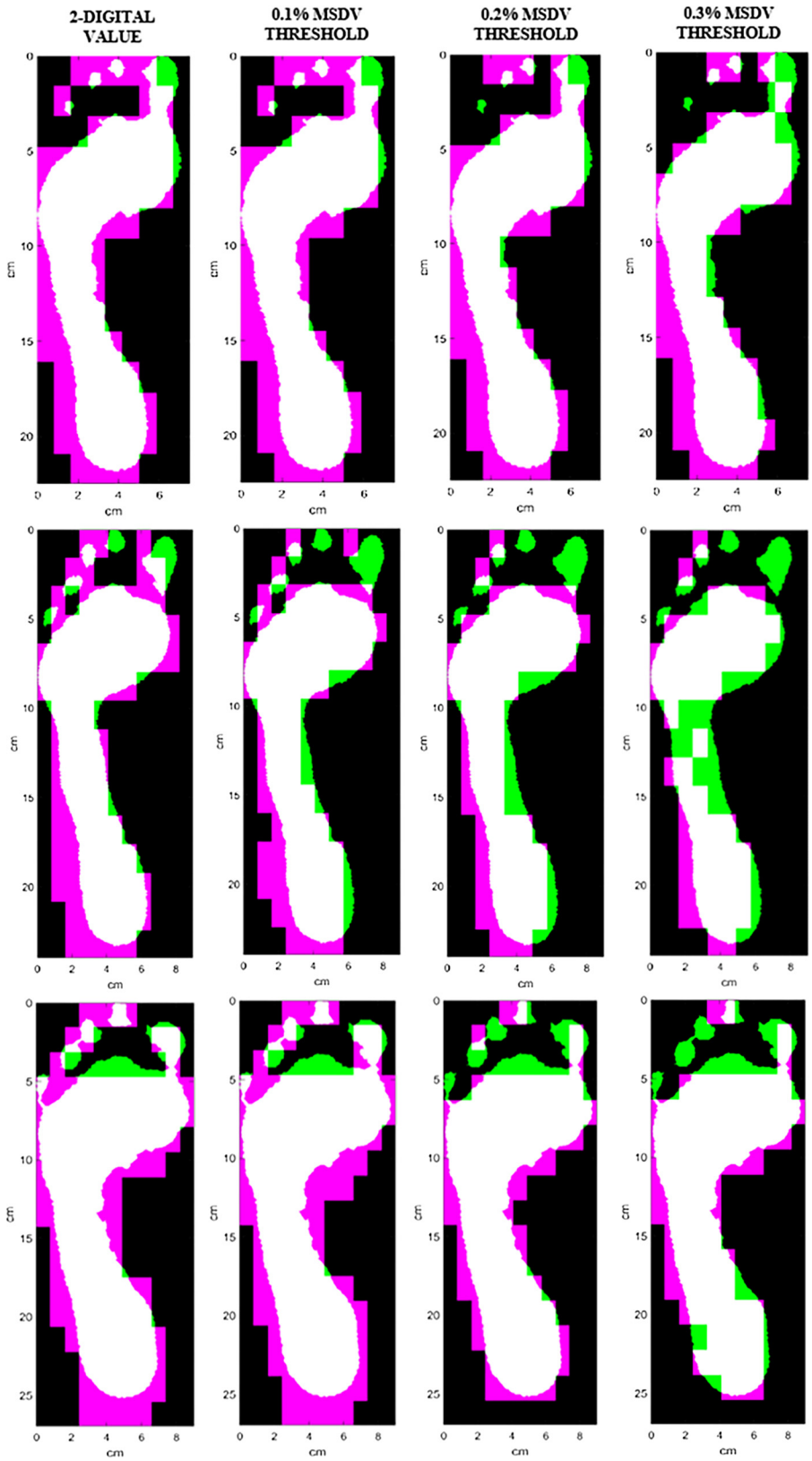

Fig. 7. Qualitative assessment between plantar contact area from insole vs. optical pedography algorithm at the same time point during mid-stance. White (areas of overlap), pink (sensors outside contact area), green (areas where sensors do not overlap reference footprint). ***Top:*** size 35; ***Middle:*** size 39; ***Bottom:*** size 43.

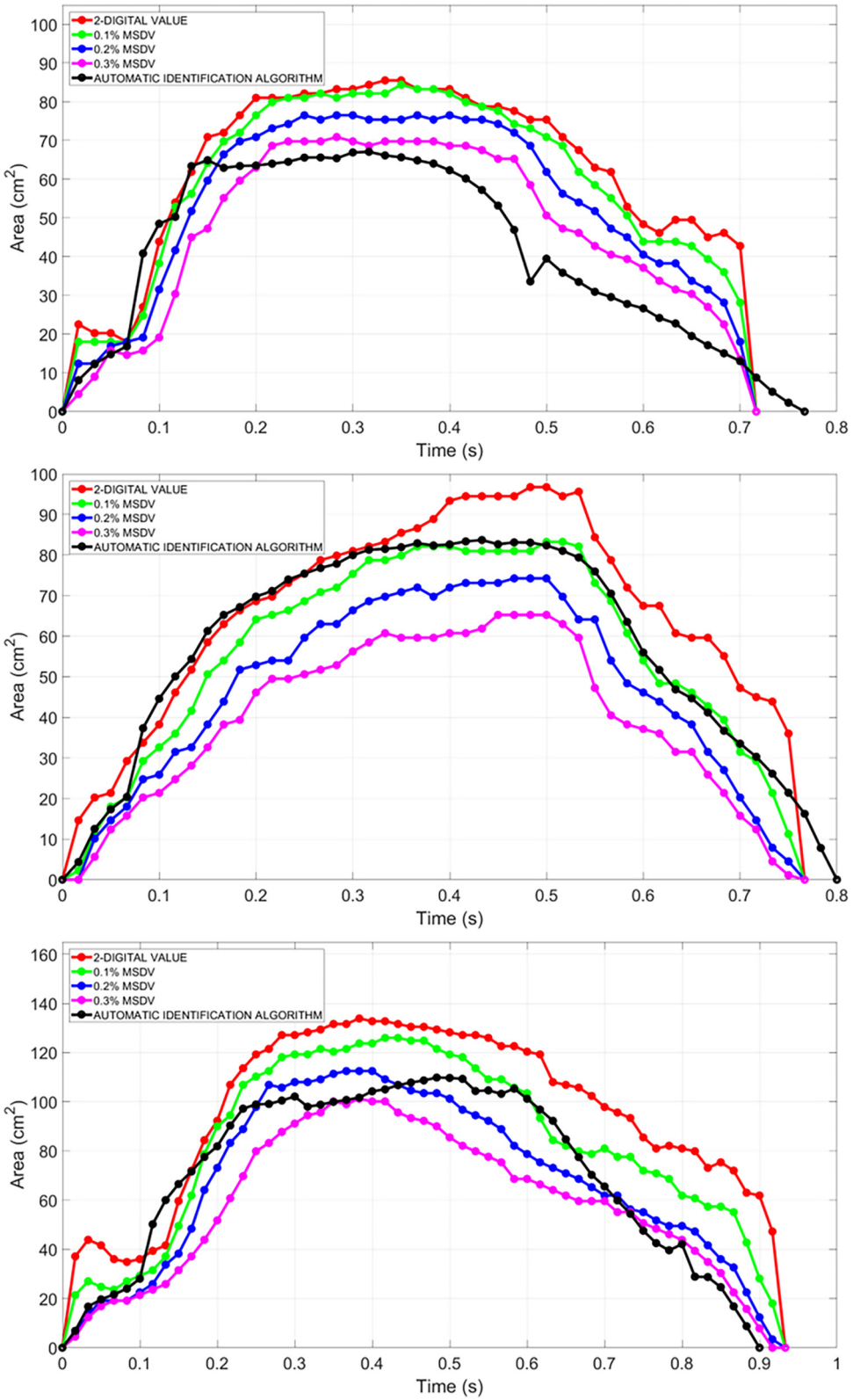

Fig. 8. ***Right:*** Area–time curve for the same participant and trials of Fig. 7. ***Top:*** size 35; ***Middle:*** size 39; ***Bottom:*** size 43.

summed digital values were converted to the normal force component (F_z) using a conversion factor specified by the manufacturer as follows (Fig. 6):

$$F_{Z,j}(N) = \sum_{i=1}^{n_i} \left(DV_{i,j} \frac{64N/cm^2}{255\ digital\ value} \right) 1.125cm^2 \quad (1)$$

where $F_{Z,j}$ is measured force at instant j

n_i is the number of sensors on insole i

$DV_{i,j}$ is the 0–255 digital value output of sensor i at instant j

A 40 N normal force threshold was used to identify heel strike and toe off [43].

Processing of Pressure-Measuring Insole Data — Two approaches were

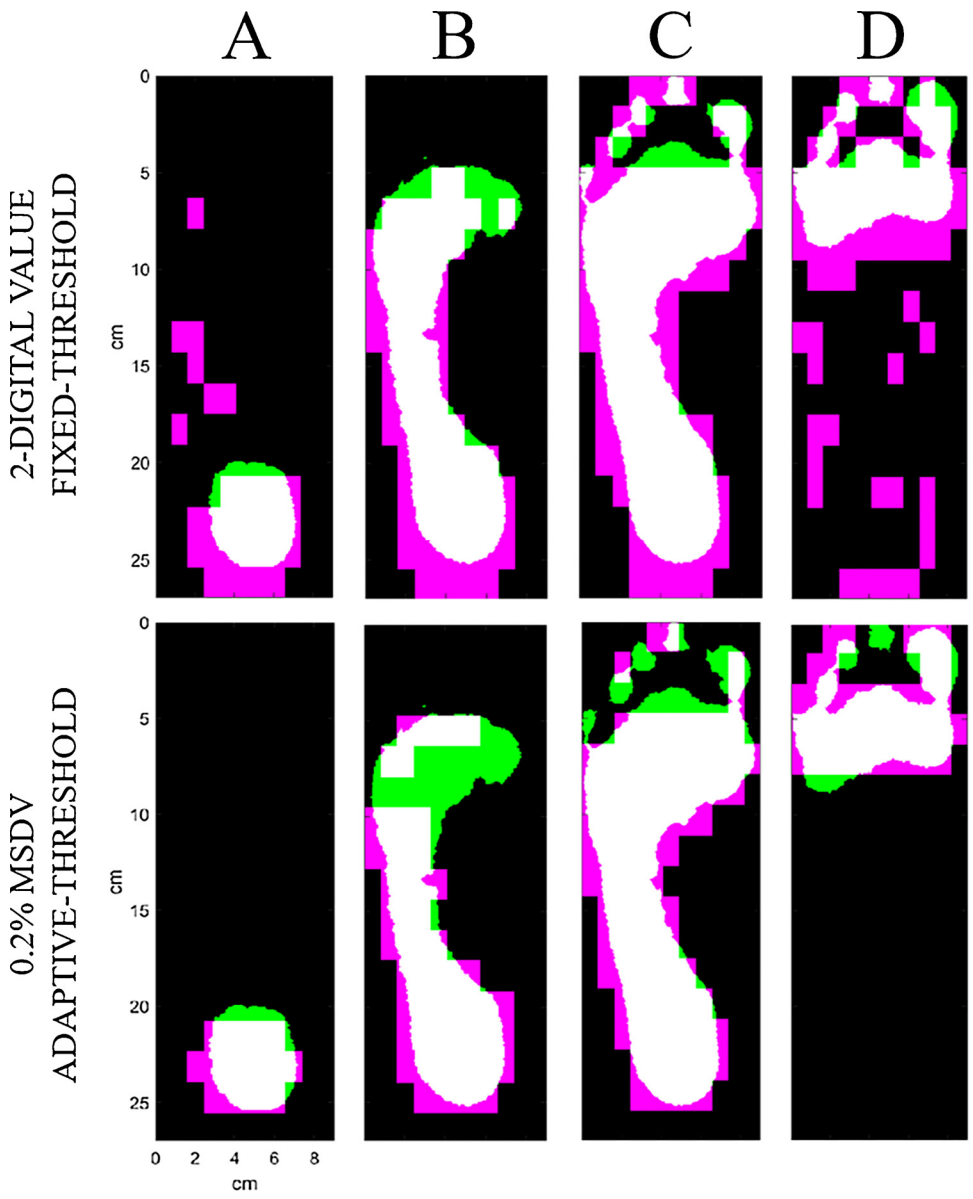

Fig. 9. ***Top:*** Qualitative assessment between plantar contact area from insole vs. optical pedography algorithm at different stages of the support phase (size 43). 2-digital value *Fixed-Threshold*; ***Bottom:*** *Adaptive-Threshold*. White (areas of overlap), pink (sensors outside contact area), green (areas where sensors do not overlap reference footprint). **A**—heel-on, **B**—full contact no toes, **C**—full contact with toes, **D**-heel-off.

used to identify sensors that were activated during contact. The first method, which was labeled, *fixed-threshold,* identified a sensor as in contact with the ground if its output was more than the digital value of 2 [32,37]. The *fixed-threshold* has limited generalizability since it is independent of the load placed on the sensors. Participants with a greater body mass (BM) or who walk at a greater velocity will likely apply higher loads on the insole. These higher loads will also increase the sensor output from partially loaded sensors not fully contributing to PA.

In the present study, an alternative to the *fixed-threshold*: a load-based *adaptive-threshold is suggested.* This technique took a percentage of the maximum sum of digital values (MSDV) of an analyzed step as the threshold. The *adaptive-threshold* would therefore increase or decrease depending on the load applied to the insole. In this work, three percentages of the MSDV were used: (0.1% 0.2%, and 0.3%) to evaluate the proposed method.

Active sensors identified using either the *fixed* or *adaptive-threshold* methods for each time instant during the stance phase were summed and converted to PA by multiplying the number of active sensors by the area of the sensor (1.125 cm^2). Area–time curves were generated for the stance phase of each trial and the areas under the area–time curves were numerically integrated and compared to the corresponding curves obtained the optical pedography. The ratio between the integral of each sensor thresholding algorithm (2-digital value, 0.1% MSDV, 0.2% MSDV, and 0.3% MSDV) and the optical pedography algorithm were calculated assuming PA symmetry between the left (*insole*) and right (*barefoot*) feet:

$$ER(\%) = \left(\frac{A_{ST}}{A_{OP}} - 1\right)100 \quad (2)$$

where *ER* is the percentage of error between the thresholding procedure and the optical pedography algorithm.

A_{ST} is the area–time curve integral when using sensor thresholding algorithm (cm^2s)

A_{OP} is the area–time curve integral when using optical pedography algorithm (cm^2s)

Table 1
Mean and standard deviation (SD) values of error ratios with respect to optical pedography by insole size. Threshold method values with ≤ ± 10% error are given in **bold**.

Insole size	Error ratio (%)			
	2-digital value (%)	0.1% MSDV (%)	0.2% MSDV (%)	0.3% MSDV (%)
35 (N = 38)	21.07 (13.18)	17.91 (12.96)	**6.53 (11.66)**	**−2.92 (9.97)**
37 (N = 113)	10.89 (8.71)	**8.71 (11.89)**	**−3.93 (10.45)**	−13.57 (9.04)
39 (N = 88)	**8.92 (12.65)**	**−7.96 (10.93)**	−23.44 (9.19)	−35.56 (7.77)
41 (N = 77)	21.44 (18.58)	**5.45 (16.44)**	−11.17 (13.55)	−23.45 (11.51)
43 (N = 58)	33.10 (20.03)	11.02 (17.25)	**−8.62 (13.96)**	−22.91 (12.47)
45 (N = 29)	69.88 (24.45)	31.79 (17.82)	**5.00 (12.69)**	−11.44 (10.92)
All (N = 403)	20.88 (22.44)	**7.31 (17.44)**	**−8.62 (15.01)**	−20.45 (14.18)

Table 2
Mean and standard deviations (SD) of error ratios with respect to optical pedography by insole size in terms of digital values. Threshold method values with ≤ ± 10% error are given in **bold**.

Insole size	Adaptive threshold value		
	0.1% MSDV (digital value)	0.2% MSDV (digital value)	0.3% MSDV (digital value)
35 (N = 38)	2.50 (0.50)	**4.52 (0.55)**	**6.63 (0.78)**
37 (N = 113)	**2.34 (0.54)**	**4.29 (0.88)**	6.27 (1.15)
39 (N = 88)	**5.45 (0.67)**	10.40 (1.19)	15.31 (1.76)
41 (N = 77)	**4.24 (0.43)**	8.02 (0.88)	11.72 (1.31)
43 (N = 58)	4.86 (0.66)	**9.37 (1.19)**	13.72 (1.68)
45 (N = 29)	5.93 (0.88)	**11.51 (1.68)**	17.03 (2.71)
All (N = 403)	**4.02 (1.48)**	**7.61 (2.89)**	11.20 (4.28)

3. Results

3.1. Qualitative analysis

The qualitative differences of PA from the different thresholds with respect to the results of the automatic identification algorithm are shown at the same time point during mid-stance for exemplar participants (Fig. 7). The associated PA curves for the same participants and trials are shown (Fig. 8). It can be observed that, in each case, the sensors in the toe region PA were underestimated with each consecutively larger *adaptive-threshold*. Pressure values are most underestimated in the toe region, since load is distributed over a smaller area [33]. This would result in high load areas, such as the heel and metatarsal regions, being less affected by greater thresholds compared to regions with the lowest load relative to body weight (mid-foot and toe region), and contributing most to total loading of the insole [44].

The PA curves in Fig. 7 show the effect of each threshold on the entire stance phase of gait for the three cases shown in Fig. 6. It is observed that the *fixed-threshold* overestimated PA especially during mid-stance when PA is largest and at heel-off when the insole is bending. The *adaptive-thresholds* reduced this error and maintained the shape of the area curve of the reference 'fixed threshold' method. However, the best-performing threshold differed for each case.

Qualitative differences in PA can be observed for all four phases of stance (heel-on, full-foot contact with no toes, full-foot contact with toes, and heel-off). As an example, a trial from a participant wearing size 43 (Fig. 9) is considered. The corresponding PA curve for this case is shown in Fig. 8 (bottom). As shown, the best performing *adaptive-threshold* for size 43 (0.2% MSDV) effectively removed erroneous sensors at heel-on and heel-off that resulted in over-estimation of PA using the *fixed-threshold* (Fig. 9). The erroneous active sensors in Fig. 9D (top row), using the *fixed-threshold*, might have been active due to bending of the insole during the heel-off phase since the bent insole might be sticking to the foot, leading to activating these sensors. The 0.2% *adaptive-threshold* shown (Fig. 9D, bottom row), appeared effective in removing these sensors from PA measurement.

3.2. Quantitative analysis

Table 1 provides the mean and standard deviation (SD) values of error ratios by insole size. Table 2 shows the mean and SD values for threshold values in digital values by insole size. The table confirms what was observed in Fig. 8 since the *fixed threshold* consistently overestimated PA for all insole sizes, with a mean error ratio of 20.88 ± 22.44%. The *adaptive thresholds*, 0.1%, 0.2%, and 0.3% MSDV had PA error ratios of 7.31 ± 17.44%, −8.62 ± 15.01%, and −20.45 ± 14.18%, respectively (Table 1). The *adaptive-thresholds* for each insole size were consistently larger than the *fixed-threshold* and increase proportionately with larger *adaptive-thresholds* and insole sizes. These results indicate that larger thresholds may be necessary to reduce PA error in individuals wearing larger insole sizes. Individuals wearing larger insole sizes tend to have higher body masses and may apply higher GRFs during walking. The *adaptive threshold* is scaled to the MSDV from the insole, that is linearly related to the GRF, and explains why size 45 has larger *adaptive-thresholds* compared to size 35 (Table 2).

The 0.3%, 0.1%, and 0.2% MSDV *adaptive-thresholds* matched the curves most closely for the cases with insole sizes 35, 39, and 43, respectively. This qualitative analysis follows the findings reported in Table 2 with sizes 35, 39, and 43 showing 0.3%, 0.1%, and 0.2% MSDV as the best performing thresholds, respectively.

4. Discussion

The purpose of this exploratory study was to examine the accuracy of an *adaptive-threshold* to reduce the PA error measured by pressure-measuring insoles. Our hypothesis that *adaptive-thresholds* would be more effective at reducing PA error compared to a *fixed-threshold* was supported. Furthermore, qualitative assessment of the results also indicated that the *adaptive-thresholds* effectively reduced noise from sensors during walking that were included as part of the PA when a *fixed-threshold* was used (Fig. 9). This is the first study to examine the effect of an *adaptive-threshold* on PA error over the entire stance phase of walking.

To assess the generalizability of the *adaptive-threshold,* results were classified using insole size (Table 1). Overall, each insole size benefited from a reduction in error ratio when using an *adaptive* vs. *fixed-threshold*. Sizes 39 and 41 benefited most from the 0.1% MSDV threshold, whereas sizes 37, 43, and 45 benefited most from using the 0.2% MSDV threshold. The smallest insole, size 35, benefited most from the most conservative threshold 0.3% MSDV. In general, the data in Table 1 follows the trend of overestimation of PA using the *fixed-threshold* with a consistent consecutive reduction in over-estimation at 0.1%, 0.2%, and 0.3% MSDV.

The findings suggest that data processing techniques are effective in reducing PA error from pressure-measuring insoles during walking. Another way to reduce PA errors from pressure measuring insoles is to increase the density of sensors. A limitation of the Medilogic® insoles used in the current study is the relatively large sensor size (1 sensor = 1.125 cm^2). This spatial resolution is nearly a fourfold reduction in the recommended spatial resolution of 1 sensor = ~25 mm^2 for pressure [33,44] and PA measurements [45]. However, the findings presented here show that the sensor size of 1.125 cm^2, combined with an *adaptive-threshold*, was sufficient to produce a reasonable estimate of PA during walking. An inherent limitation of low sensor spatial

resolution is the greater potential for overestimation of the PA due to partial loading of sensors along the perimeter of the footprint [13]. Furthermore, when walking; insole bending, sticking of the insole to the foot, and hysteresis of sensors introduce noise in PA measurements that may not be reduced with sensor size reduction. The proposed *adaptive-threshold* effectively reduces sensor noise when measuring the PA during walking

Lastly, the *adaptive-threshold* adapts to the maximal load applied to the insole and may be more effective at reducing PA error in high-load regions (ex. heel and metatarsals) compared to low-load regions (ex. mid-foot and toes) on the foot. In the current study, qualitative assessment showed that sensors in the toe region may be disproportionately removed using the *adaptive-threshold*. Applying a region-specific adaptive-threshold may therefore improve accuracy of PA measurement when using pressure-measuring insoles, since forces differ across the anatomical structures of the foot [33,44].

4.1. Limitations

A limitation of the current study is that the effect of foot types on PA error when using the various thresholds was not examined. Furthermore, the effect of foot type on the validity of the Automated Identification Algorithm was also not examined [40]. While we did not assess the effects of different foot types on the performance of the algorithm in our previous validation study, we were able to show that the algorithm produced acceptable results for most participants (N = 42) showing generalizability regardless of foot type. Furthermore, the previous validation study [40] and the current study used data collected from the same participants in the same sessions. In our previous study [40] on the validity of an Automated Identification Algorithm, only video data recorded from the right foot of the participants were processed to derive PA, whereas the current study analyzed PA from both the right (video) and left (pressure-measuring insole) feet using two separate techniques.

Another limitation of the study is that PA during walking was assumed to be symmetrical between the left and right feet. However, despite this limitation, only healthy participants with non-pathological gait or observable foot deformities were recruited. Any PA differences between the feet were likely insignificant relative to PA errors from the measurement insole. However, the authors cannot rule out the possibility of altered PA of the left foot due to wearing the measurement insole.

Finally, the *adaptive-threshold* algorithm proposed in the current study did not consider the foot region the sensor was located in. This might have resulted in a loss of sensors in low-load regions leading to an underestimation of PA using the *adaptive-threshold*.

5. Conclusions

This is the first study to: (1) quantify PA error over the entire stance phase of walking using pressure-measuring insoles, and (2) examine the effectiveness of an *adaptive-threshold* technique to reduce PA error. The results from the current study demonstrate that PA error from pressure-measuring insoles can be reduced from over 20% to less than 10% using load-based *adaptive-thresholds*. The findings presented also show that a sensor size of 1.125 cm^2 provides a reasonable estimate of plantar contact area during walking. While these recommendations were obtained using Medilogic® insoles, future studies should examine the generalizability of the *adaptive-threshold* proposed here to other pressure-measuring devices.

Brief summary

What is already known:

- The current method to identify the plantar contact area using pressure-measuring insoles is based on arbitrarily-chosen *fixed-threshold* values of the sensors output.
- However, plantar contact errors over the entire stance phase of walking using a *fixed-threshold* method was not quantified.
- Furthermore, the *fixed-threshold* method does not account for variation in insole sizes.

What this study adds:

- This study showed that identification of the plantar contact area during walking using a *fixed-threshold* produced unacceptable results.
- We proposed an *adaptive-threshold* based on the percentage of the maximum sum of digital values (MSDV) during the analyzed step.
- Experiments showed that using 0.1% and 0.2% of the MSDV substantially reduced plantar contact area error compared to the commonly used *fixed-threshold* method.

Conflict of interest

None.

References

[1] Dunn JE, Link CL, Felson DT, Crincoli MG, Keysor JJ, McKinlay JB. Prevalence of food and ankle conditions in a multiethnic community sample of older adults. Am J Epidemiol 2004;159:491–8. https://doi.org/10.1093/aje/kwh071.

[2] Ledoux WR, Shofer JB, Ahroni JH, Smith DG, Sangeorzan BJ, Boyko EJ. Biomechanical differences among pes cavus neutrally aligned, and pes planus feet in subjects with diabetes. Foot Ankle Int 2003;24:845–50. https://doi.org/10.1177/107110070302401107.

[3] Tong JWK, Kong PW. Association between foot type and lower extremity injuries: systematic literature review with meta-analysis. J Orthop Sport Phys Ther 2013;43:700–14. https://doi.org/10.2519/jospt.2013.4225.

[4] Burns J, Crosbie J, Hunt A, Ouvrier R. The effect of pes cavus on foot pain and plantar pressure. Clin Biomech 2005;20:877–82. https://doi.org/10.1016/j.clinbiomech.2005.03.006.

[5] Kosashvili Y, Fridman T, Backstein D, Safir O, Bar Ziv Y. The correlation between pes planus and anterior knee or intermittent low back pain. Foot Ankle Int 2008;29:910–3. https://doi.org/10.3113/FAI.2008.0910.

[6] Fernandez-Seguin LM, Diaz Mancha JA, Sanchez Rodriguez R, Escamilla Martinez E, Gomez Martin B, Ramos Ortega J. Comparison of plantar pressures and contact area between normal and cavus foot. Gait Posture 2014;39:789–92. https://doi.org/10.1016/j.gaitpost.2013.10.018.

[7] Bok SK, Lee H, Kim BO, Ahn S, Song Y, Park I. The effect of different foot orthosis inverted angles on plantar pressure in children with flexible flatfeet. PLoS One 2016;11:1–10. https://doi.org/10.1371/journal.pone.0159831.

[8] Mathieson I, Upton D, Birchenough A. Comparison of footprint parameters calculated from static and dynamic footprints. Foot 1999;9:145–9. https://doi.org/10.1054/foot.1999.0544.

[9] Razeghi M, Batt ME. Foot type classification: a critical review of current methods. Gait Posture 2002;15:282–91. https://doi.org/10.1016/S0966-6362(01)00151-5.

[10] Sawacha Z, Guarneri G, Cristoferi G, Guiotto A, Avogaro A, Cobelli C. Integrated kinematics-kinetics-plantar pressure data analysis: a useful tool for characterizing diabetic foot biomechanics. Gait Posture 2012;36:20–6. https://doi.org/10.1016/j.gaitpost.2011.12.007.

[11] Giacomozzi C, Stebbins JA. Anatomical masking of pressure footprints based on the Oxford Foot Model: validation and clinical relevance. Gait Posture 2017;53:131–8. https://doi.org/10.1016/j.gaitpost.2016.12.022.

[12] Cavanagh PR, Rodgers MM. The arch index: a useful measure from footprints. J Biomech 1987;20:547–51. https://doi.org/10.1016/0021-9290(87)90255-7.

[13] Urry SR, Wearing SC. The accuracy of footprint contact area measurements: relevance to the design and performance of pressure platforms. Foot 2001;11:151–7. https://doi.org/10.1054/foot.2001.0684.

[14] Urry SR, Wearing SC. A comparison of footprint indexes calculated from ink and electronic footprints. J Am Podiatr Med Assoc 2001;91:203–9.

[15] Urry SR, Wearing SC. Arch indexes from ink footprints and pressure platforms are different. Foot 2005;15:68–73. https://doi.org/10.1016/j.foot.2005.02.001.

[16] Fascione JM, Crews RT, Wrobel JS. Dynamic footprint measurement collection technique and intrarater reliability. J Am Podiatr Med Assoc 2012;102:130–8. https://doi.org/10.7547/1020130.

[17] Zuil-Escobar JC, Martínez-Cepa CB, Martín-Urrialde JA, Gómez-Conesa A. Reliability and accuracy of static parameters obtained from ink and pressure platform footprints. J Manipulative Physiol Ther 2016;39:510–7. https://doi.org/10.1016/j.jmpt.2016.07.005.

[18] Su KH, Kaewwichit T, Tseng CH, Chang CC. Automatic footprint detection approach for the calculation of arch index and plantar pressure in a flat rubber pad. Multimed Tools Appl 2016;75:9757–74. https://doi.org/10.1007/s11042-015-2796-x.

[19] Garrow AP, Van Schie CHM, Boulton AJM. Efficacy of multilayered hosiery in reducing in-shoe plantar foot pressure in high-risk patients with diabetes. Diabetes Care 2005;28:2001–6. https://doi.org/10.2337/diacare.28.8.2001.
[20] Cavanagh PR, Ae M. A technique for the display of pressure distributions beneath the foot. J Biomech 1980;13:69–75. https://doi.org/10.1016/0021-9290(80)90180-3.
[21] Chu WC, Lee SH, Chu W, Wang TJ, Lee MC. The use of arch index to characterize arch height: a digital image processing approach. IEEE Trans Biomed Eng 1995;42:1088–93. https://doi.org/10.1109/10.469375.
[22] Lidstone DE, Porcher LM, Deberardinis J, Dufek JS, Trabia MB. Concurrent validity of an automatic technique to calculate plantar contact area at mid-stance during Gait. 41st annual meeting of the american society of biomechanics 2017.
[23] Gefen A, Megido-Ravid M, Itzchak Y, Arcan M. Biomechanical analysis of the three-dimensional foot structure during Gait: a basic tool for clinical applications. J Biomech Eng 2000;122:630. https://doi.org/10.1115/1.1318904.
[24] Shah SR, Patil KM. Processing of foot pressure images and display of an advanced clinical parameter PR in Diabetic Neuropathy. Proceedings of the 2005 IEEE 9th International conference on rehabilitation robotics 2005;vol. 2005:414–7. https://doi.org/10.1109/ICORR. 2005.1501131.
[25] Mora M, Sbarbaro D. A Robust Footprint Detection Using Color Images and Neural Networks. Elements 2016;2005:311–8. https://doi.org/10.1007/11578079_33.
[26] Aruntammanak W, Aunhathaweesup Y, Wongseree W, Leelasantitham A, Kiattisin S. Diagnose flat foot from foot print image based on neural network. BMEiCON 2013 — 6th Biomedical Engineering International Conference 2013. https://doi.org/10.1109/BMEiCon.2013.6687684.
[27] Gutiérrez-Vilahú L, Massó-Ortigosa N, Rey-Abella F, Costa-Tutusaus L, Guerra-Balic M. Reliability and Validity of the footprint assessment method using photoshop CS5 software. J Am Podiatr Med Assoc 2015;105:226–32. https://doi.org/10.7547/15-012.
[28] Siddiqui HUR, Spruce M, Alty SR, Dudley S. Automated peripheral neuropathy assessment using optical imaging and foot anthropometry. IEEE Trans Biomed Eng 2015;62:1911–7. https://doi.org/10.1109/TBME.2015.2407056.
[29] Buchelly FJ, Mayorca D, Ballarin V, Pastore J. Digital image processing techniques applied to pressure analysis and morphological features extraction in footprints. J Phys Conf Ser 2016;70:5. https://doi.org/10.1088/1742-6596/705/1/012020.
[30] Rodolfo Maestre-Rendon J, Rivera-Roman TA, Sierra-Hernandez JM, Cruz-Aceves I, Contreras-Medina LM, Duarte-Galvan C, et al. Low computational-cost footprint deformities diagnosis sensor through angles, dimensions analysis and image processing techniques. Sensors (Switzerland) 2017;1:7. 10.3390/s17112700.
[31] Titianova EB, Mateev PS, Tarkka IM. Footprint analysis of gait using a pressure sensor system. J Electromyogr Kinesiol 2004;14:275–81. https://doi.org/10.1016/S1050-6411(03)00077-4.
[32] Price C, Parker D, Nester C. Validity and repeatability of three in-shoe pressure measurement systems. Gait Posture 2016;46:69–74. https://doi.org/10.1016/j.gaitpost.2016.01.026.
[33] Davis BL, Cothren RM, Quesada P, Hanson SB, Perry JE. Frequency content of normal and diabetic plantar pressure profiles: implications for the selection of transducer sizes. J Biomech 1996;29:979–83. https://doi.org/10.1016/0021-9290(95)00116-6.
[34] Koch M, Lunde LK, Ernst M, Knardahl S, Veiersted KB. Validity and reliability of pressure-measurement insoles for vertical ground reaction force assessment in field situations. Appl Ergon 2016;53:44–51. https://doi.org/10.1016/j.apergo.2015.08.011.
[35] Ghanem A, DeBerardinis J, Trabia M, Dufek J, Lidstone D. Identification of hysteresis behavior of pressure-measuring insoles. 2017 Summer biomechanics, bioengineering, and biotransport conference. 2017.
[36] Fascione JM, Crews RT, Wrobel JS. Association of footprint measurements with plantar kinetics: a linear regression model. J Am Podiatr Med Assoc 2014;104:125–33. https://doi.org/10.7547/0003-0538-104.2.125.
[37] Nouman M, Leelasamran W, Chatpun S. Effectiveness of total contact orthosis for plantar pressure redistribution in neuropathic diabetic patients during different walking activities. Foot Ankle Int 2017;38:901–8. https://doi.org/10.1177/1071100717704427.
[38] Noraxon Medilogic Wireless Foot Pressure Measurement System n.d.:4. https://www.noraxon.com/products/pressure-and-force-measurement-technology/medilogic-insoles/. [Accessed 25 September 2017].
[39] Kasarova S, Sultanova N, Ivanov C, Nikolov I. Analysis of the dispersion of optical plastic materials. Opt Mater (Amst) 2007;29:1481–90. https://doi.org/10.1016/j.optmat.2006.07.010.
[40] Lidstone DE, Porcher LM, DeBerardinis J, Dufek JS, Trabia MB. Concurrent validity of an automated footprint detection algorithm to measure plantar contact area during walking. J Am Podiatr Med Assoc 2018. [in press].
[41] Mohd Said A, Justine M, Manaf H. Plantar pressure distribution among older persons with different types of foot and its correlation with functional reach distance. Scientifica (Cairo) 2016;2016:1–7. https://doi.org/10.1155/2016/8564020.
[42] DeBerardinis J, Dufek JS, Trabia MB, Lidstone DE. Assessing the validity of pressure-measuring insoles in quantifying gait variables. J Rehabil Assist Technol Eng 2018:1–12. Special Co.
[43] Riley PO, Paolini G, Croce UD, Paylo KW, Kerrigan DC. A kinematic and kinetic comparison of overground and treadmill walking in healthy subjects. Gait Posture 2006;26:17–24. https://doi.org/10.1016/j.clinbiomech.2009.09.002.
[44] Wearing SC, Urry SR, Smeathers JE. Ground reaction forces at discrete sites of the foot derived from pressure plate measurements. Foot Ankle Int 2001;22:653–61. https://doi.org/10.1177/107110070102200807.
[45] Urry SRR, Wearing SCC. The accuracy of footprint contact area measurements: relevance to the design and performance of pressure platforms. Foot 2001;11:151–7. https://doi.org/10.1054/foot.2001.0684.